Environ. Sci. Technol. **2005**, *39,* 7147−7153

Competing Fe(II)-Induced Mineralization Pathways of Ferrihydrite

COLLEEN M. HANSEL,*,† SHAWN G. BENNER,‡ AND SCOTT FENDORF*,†

Department of Geological and Environmental Sciences, Stanford University, Stanford, California 94305, and Department of Geosciences, Boise State University, Boise, Idaho 83725

Owing to its high surface area and intrinsic reactivity, ferrihydrite serves as a dominant sink for numerous metals and nutrients in surface environments and is a potentially important terminal electron acceptor for microbial respiration. Introduction of Fe(II), by reductive dissolution of Fe(III) minerals, for example, converts ferrihydrite to Fe phases varying in their retention and reducing capacity. While Fe(II) concentration is the master variable dictating secondary mineralization pathways of ferrihydrite, here we reveal that the kinetics of conversion and ultimate mineral assemblage are a function of competing mineralization pathways influenced by pH and stabilizing ligands. Reaction of Fe(II) with ferrihydrite results in the precipitation of goethite, lepidocrocite, and magnetite. The three phases vary in their precipitation extent, rate, and residence time, all of which are primarily a function of Fe(II) concentration and ligand type (Cl, SO_4, CO_3). While lepidocrocite and goethite precipitate over a large Fe(II) concentration range, magnetite accumulation is only observed at surface loadings greater than 1.0 mmol Fe(II)/g ferrihydrite (in the absence of bicarbonate). Precipitation of magnetite induces the dissolution of lepidocrocite (presence of Cl) or goethite (presence of SO_4), allowing for Fe(III)-dependent crystal growth. The rate of magnetite precipitation is a function of the relative proportions of goethite to lepidocrocite; the lower solubility of the former Fe (hydr)oxide slows magnetite precipitation. A one unit pH deviation from 7, however, either impedes (pH 6) or enhances (pH 8) magnetite precipitation. In the absence of magnetite nucleation, lepidocrocite and goethite continue to precipitate at the expense of ferrihydrite with near complete conversion within hours, the relative proportions of the two hydroxides dependent upon the ligand present. Goethite also continues to precipitate at the expense of lepidocrocite in the absence of chloride. In fact, the rate and extent of both goethite and magnetite precipitation are influenced by conditions conducive to the production and stability of lepidocrocite. Thus, predicting the secondary mineralization of ferrihydrite, a process having sweeping influences on contaminant/nutrient dynamics, will need to take into consideration kinetic restraints and transient precursor phases (e.g., lepidocrocite) that influence ensuing reaction pathways.

Introduction

Ferrihydrite is a common Fe(III) (hydr)oxide in soils and sediments undergoing fluctuating redox conditions (*1*). Due to its high surface area and intrinsic reactivity, ferrihydrite serves as a dominant sink for numerous metals (e.g., As) and nutrients (e.g., P). Ferrihydrite is also considered the most (bio)available Fe(III) (hydr)oxide for dissimilatory iron-reducing bacteria (DIRB) and thus greatly influences the global cycling of carbon (*2*). A number of Fe-bearing phases, encompassing a spectrum of reactivities and reduction potentials, have been observed following the bacterial reduction of ferrihydrite (*3*−*6*). Considering the importance of Fe phases in nutrient/contaminant retention coupled with the reducing capacity of Fe(II) species, Fe(II)-induced mineralization pathways of ferrihydrite have environmental implications for the fate and transport of both nutrients and contaminants.

Ferrihydrite is thermodynamically unstable with respect to goethite, lepidocrocite, and hematite under oxygenated conditions (*1*). The kinetics of ferrihydrite conversion, however, are slow in the absence of catalysts. Strong reductants (e.g., cysteine) may induce interfacial electron transfer to structural Fe(III), thus stimulating dissolution and subsequent reprecipitation as a thermodynamically more stable phase (*7*). Due to its strong reducing capacity, ferrous Fe induces the dissolution and subsequent conversion of ferrihydrite (*6*, *8*−*10*). Under advective flow, we have consistently observed the rapid and near complete conversion of 2-line ferrihydrite-coated sand to goethite (minor product) and magnetite (major product; 1.0 mmol Fe(II)/g ferrihydrite) upon dissimilatory Fe(III) reduction within both a bicarbonate buffered (10 mM) and an artificial groundwater medium supplemented with 3 mM lactate (*6*, *11*, *12*). The secondary mineralization of ferrihydrite occurs via a coupled biotic-abiotic mechanism, involving the Fe(II)-induced conversion of ferrihydrite to goethite and magnetite. The operating secondary mineralization pathways following reductive dissolution of ferrihydrite at a given pH are governed principally by Fe(II) concentration and flux (*5*, *6*). With increasing initial Fe(II) concentration, a mineral phase progression is observed from unaltered ferrihydrite to goethite/lepidocrocite to goethite/magnetite (see Supporting Information Figure S1). The addition of as little as 40 μM Fe(II) (∼0.1 mmol Fe(II)/g ferrihydrite) leads to the conversion of nearly half of the ferrihydrite to goethite and lepidocrocite within 9 d. While goethite precipitation occurs over a large Fe(II) concentration range, magnetite accumulation is only observed at surface loadings greater than 1.0 mmol Fe(II)/g ferrihydrite (derived from aqueous concentrations exceeding 0.3 mM). Goethite concentrations reach a maximum of ca. 40% (mol % Fe) but are lower (ca. 25%) at Fe(II) concentrations (>1.0 mmol Fe(II)/g ferrihydrite) conducive for magnetite precipitation. Similarly, lepidocrocite concentrations peak at ca. 58% but become negligible at high Fe(II) concentrations. Addition of Fe(II) concentrations exceeding 1.5 mM do not alter the final mineral secondary phases even though ca. 10% ferrihydrite and 25% goethite are still present. Preservation of ferrihydrite and lack of conversion to either magnetite or goethite suggests that heterogeneous secondary precipitation on ferrihydrite may result in a small fraction being occluded and thus not

* Address correspondence to either author. Phone: (650)723-4152 (C.M.H.); (650)723-5238 (S.F.). E-mail: hansel@pangea.stanford.edu (C.M.H.); fendorf@pangea.stanford.edu (S.F.).
† Stanford University.
‡ Boise State University.

10.1021/es050666z CCC: $30.25
Published on Web 08/18/2005

readily accessible for further reaction (*6*). Incomplete ferrihydrite reduction and conversion is consistently observed both upon abiotic reaction with Fe(II) and via dissimilatory iron reduction in the absence of a metal chelator (*3*, *5*, *10*, *11*, *13*, *14*).

The factors influencing Fe(II)-induced secondary mineralization of ferrihydrite, however, remain elusive. Accordingly, this research investigates geochemical controls on the extent, rate, and mechanisms of abiotic Fe(II)-induced transformation of 2-line ferrihydrite. The influence of pH, Fe(II) concentration, and type of counterions (Cl, SO_4, CO_3) on coupled and competing mineralization pathways is investigated. While Fe(II) concentration is the master variable dictating secondary mineralization pathways following reductive dissolution of ferrihydrite, here we reveal that the kinetics of conversion and ultimate mineral assemblage are a function of competing mineralization pathways that are also governed by pH and stabilizing ligands.

Materials and Methods

Synthetic Fe-Coated Sands. Two-line ferrihydrite, goethite, and lepidocrocite were synthesized following the procedures by Schwertmann and Cornell (2000) and coated on quartz sand as described in detail previously (*6*, *12*). After the Fe (hydr)oxide was washed by either centrifugation or dialysis, quartz sand was added to the suspension. The coated sand was dried at 20 °C under convection while the mixture was periodically stirred for 4 d and then resaturated with water and heat sterilized. Both X-ray diffraction (XRD) and X-ray absorption spectroscopy (XAS) verified the presence and purity of the Fe (hydr)oxide phases. Surface area analysis was conducted on a Beckman-Coulter SA3100 analyzer using a single-point isotherm with N_2(g) as the adsorbate on He (24 h) purged samples. The surface area of the 2-line ferrihydrite-, goethite-, and lepidocrocite-coated sand is 2.6, 1.0, and 0.80 $m^2\ g^{-1}$, respectively. The uncoated Si sand has a surface area of $<0.1\ m^2\ g^{-1}$. The concentration of Fe on the sand is 10 mg g^{-1} (1 wt % Fe).

Experimental Procedures. Reactions were performed in 125 mL serum vials containing either ferrous chloride or ferrous sulfate and 1.35 g of Fe(III) (hydr)oxide-coated sand (1% Fe by weight) within anaerobic PIPES (1,4-piperazinediethanesulfonic acid) or bicarbonate (10 mM) buffer (pH 7.2). The role of Fe(II) concentration and ligand type on secondary mineralization was investigated by reacting 0.2 and 2.0 mM ferrous chloride and ferrous sulfate with ferrihydrite. Kinetic studies were performed by running a series of reaction vials and sacrificing vials at each time point. Vials were equilibrated and maintained at pH 7.2 under an N_2 (PIPES) or 90% N_2/10% CO_2 (bicarbonate) atmosphere and gently shaken to minimize diffusion effects. Samples were extracted anaerobically using a sterile syringe and analyzed for pH and aqueous Fe(II) concentration. All reactions were performed in duplicate.

Sampling and Analysis. Aqueous concentrations of major dissolved constituents and pH were measured as a function of time. Production of soluble Fe(II) was monitored spectrophotometrically at 562 nm using the ferrozine assay (*15*). Total dissolved Fe was determined by inductively coupled plasma optical emission spectroscopy (ICP-OES).

Solids intended for X-ray absorption spectroscopic analyses were dried in the anaerobic glovebox, mounted on a Teflon plate, and sealed with Kapton polymide film to prevent moisture loss and oxidation while minimizing X-ray adsorption. The speciation and structural environment of Fe were determined using X-ray absorption spectroscopy (XAS) as described previously (*6*). Briefly, a set of reference standards for Fe (for more details, see ref *6*) was utilized to perform linear combination k^3-weighted EXAFS spectral fitting using the EXAFSPAK module DATFIT (*16*). Linear combinations of empirical model spectra were optimized where the only adjustable parameters were the fractions of each model compound contributing to the fit. Fits were optimized by minimizing the residual, defined as the normalized root square difference between the data and the fit. The accuracy of linear combination Fe EXAFS fits (qualitative and quantitative) was investigated previously (*6*). Fits are within ±5 of actual mole percentages using the k-range $1-14\ Å^{-1}$. The detection limit for minor constituents is ca. 5%.

Mineral associations were obtained via high-resolution transmission electron microscopy (HRTEM). Reacted Fe (hydr)oxide-coated sands were embedded in LR white resin and anaerobically sectioned on a microtome. Samples were stored anaerobically and were only exposed to oxygen during transfer (<1 min) to the high-vacuum sample chamber of the TEM. Imaging and analyses were performed using a JEOL 2010 high-resolution TEM, which was equipped with a LaB_6 filament as an electron source and operated at 200 kV with 1.9 Å point-to-point resolution.

Results

Role of Fe(II) Concentration. The impact of Fe(II) concentration on the extent and rate of ferrihydrite mineralization was investigated at 0.2 and 2.0 mM Fe(II) (~0.67 and 6.7 mmol Fe(II)/g ferrihydrite) at circumneutral pH, concentrations below and above the threshold required for magnetite precipitation (~1.0 mmol Fe(II)/g ferrihydrite), respectively. Increasing the concentration of $FeCl_2$ from 0.2 to 2.0 mM results in a decrease in the extent of ferrihydrite transformation from 94% (6% ferrihydrite remaining) to 79% (21% ferrihydrite remaining) after 132 h of reaction (Figure 1; Table 1). While the extent of ferrihydrite conversion decreases, the rate of secondary mineralization substantially increases. Within the first 2 h, ferrihydrite conversion increases from 16% to 70% by increasing the Fe(II) concentration from 0.2 to 2.0 mM (Figure 1). The rates of both lepidocrocite and goethite precipitation are nearly an order of magnitude faster at higher initial Fe(II) concentrations (Table 2). Yet, the extent of lepidocrocite accumulation is lower at higher Fe(II) levels, suggesting that continued lepidocrocite precipitation is impeded by the formation of, or conditions leading to, goethite and/or magnetite. Over time, magnetite continues to accumulate seemingly at the expense of lepidocrocite; concentrations of ferrihydrite and goethite are constant following ca. 30 h of reaction (Figure 1). Reaction of 2 mM $FeCl_2$ with lepidocrocite-coated sand (192 h), however, does not result in conversion to magnetite (see Supporting Information Table S1), suggesting that Fe(II) reaction with lepidocrocite does not result in structural conversion of lepidocrocite to magnetite.

The impact of Fe(II) concentration on the extent and rate of ferrihydrite mineralization was also investigated at 0.2 and 2.0 mM Fe(II) using $FeSO_4$ as the Fe(II) source (pH = 7.2). As observed for $FeCl_2$, increasing the concentration of $FeSO_4$ from 0.2 to 2.0 mM decreases the extent but enhances the rate of ferrihydrite dissolution and conversion after 132 h (Table 2; Figure 1). At lower Fe(II) concentrations, the rate of lepidocrocite precipitation exceeds that of goethite, allowing for an initially higher concentration of the former (Table 1; Figure 1). Following ca. 30 h, however, the proportions of goethite and lepidocrocite are equivalent and further conversion is not observed. Increasing the initial Fe(II) concentration to 2 mM results in an increased rate and extent of goethite precipitation. Lepidocrocite is only detected at 2 h, suggesting that the rate of lepidocrocite precipitation and subsequent dissolution are also enhanced at higher Fe(II) concentrations (Figure 1). We propose that lepidocrocite precipitation peaked and nearly completely converted to goethite within the first 2 h. Addition of 2 mM $FeSO_4$ to lepidocrocite-coated sand (192 h) results in ap-

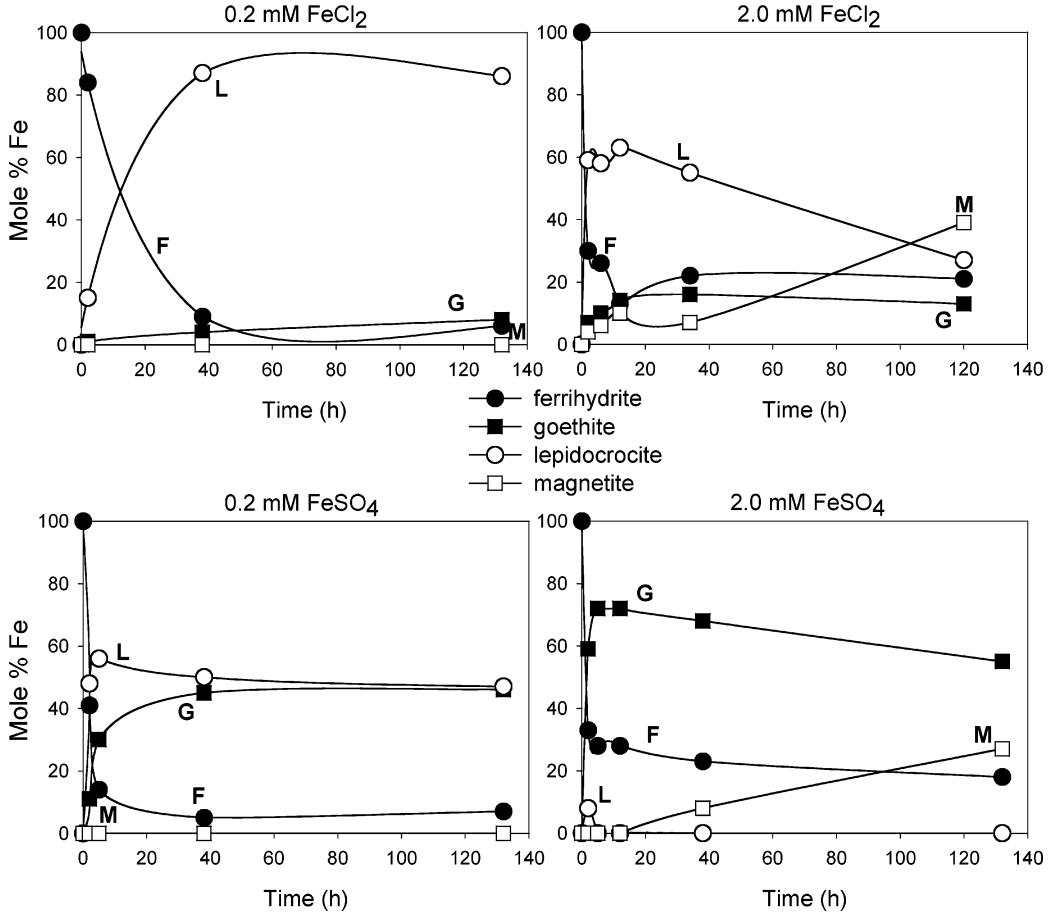

FIGURE 1. Rates of ferrihydrite (F) conversion to the secondary phases goethite (G), lepidocrocite (L), and magnetite (M) as a function of Fe(II) concentration and ligand (10 mM PIPES, pH 7.2). Percentages (±5 mol %) were determined from linear combination fits of k^3-weighted Fe EXAFS spectra ($k = 1-14$) with a detection limit of ca. 5%.

TABLE 1. Fe(II)-Induced Conversion of 2-Line Ferrihydrite as a Function of Fe(II) Concentration and Complexing Ligand Following 132 h of Reaction

Fe(II) (mM)	ligand	mol % Fe			
		ferrihydrite	goethite	lepidocrocite	magnetite
		PIPES Buffer			
0.2	Cl	6	8	86	0
0.2	SO_4	7	46	47	0
2.0	Cl	21	13	27	39
2.0	SO_4	18	55	0	27
		Bicarbonate Buffer[a]			
0.2	SO_4	44	56	0	0
2.0	SO_4	30	70	0	0

[a] 10 mM bicarbonate buffer.

TABLE 2. Minimum Initial (0 to 2−5 h) Precipitation Rates of Secondary Fe Phases upon Fe(II)-Induced Conversion of 2-Line Ferrihydrite as a Function of Fe(II) Concentration and Complexing Ligand

	0.2 mM		2.0 mM	
	Cl	SO_4	Cl	SO_4
	mol Fe s^{-1}			
lepidocrocite	5×10^{-06}	2×10^{-05}	2×10^{-05}	3×10^{-06} [b]
goethite	3×10^{-07}	4×10^{-06}	2×10^{-06}	2×10^{-05}
magnetite	nd[a]	nd	1×10^{-06}	1×10^{-07}
	mol Fe m^{-2} s^{-1}			
lepidocrocite	1×10^{-09}	5×10^{-09}	6×10^{-09}	8×10^{-10}
goethite	1×10^{-10}	1×10^{-09}	7×10^{-10}	6×10^{-09}
magnetite	nd[a]	nd[a]	4×10^{-10}	4×10^{-11}

[a] nd = not detected. [b] Rate underestimated; maximum conversion prior to first sampling.

proximately one-third conversion of lepidocrocite to goethite (see Supporting Information Table S1).

As observed for lepidocrocite (for 2 mM $FeCl_2$), goethite accumulation halts upon the precipitation of magnetite (Figure 1). Magnetite is not observed upon reaction of 2 mM $FeSO_4$ with goethite-coated sand, indicating that the decline in goethite levels is not a result of structural conversion to magnetite (see Supporting Information Table S1; ref *12*).

Role of Ligands. Steady-state mineral assemblages following abiotic reaction of ferrous Fe with ferrihydrite are impacted by ligand (Cl, SO_4, CO_3) type at circumneutral pH (Table 1). Upon addition of 0.2 mM ferrous Fe, chloride favors the conversion of ferrihydrite to lepidocrocite, while sulfate supports both goethite and lepidocrocite (in equal proportions after 132 h) (Figure 1). While the precipitation and stabilization of lepidocrocite are diminished in the absence of chloride, lepidocrocite is not completely converted to goethite and instead the two iron hydroxides exist in equal proportions. Following reaction of 2.0 mM ferrous Fe, magnetite is observed regardless of the ligand present. However, at higher Fe(II) concentrations, lepidocrocite is only observed following 132 h of reaction in the presence of chloride. In fact, magnetite concentrations continue to increase at the expense of lepidocrocite, such that lepidocrocite is completely consumed within 9 d of reaction (see Supporting Information Figure S1).

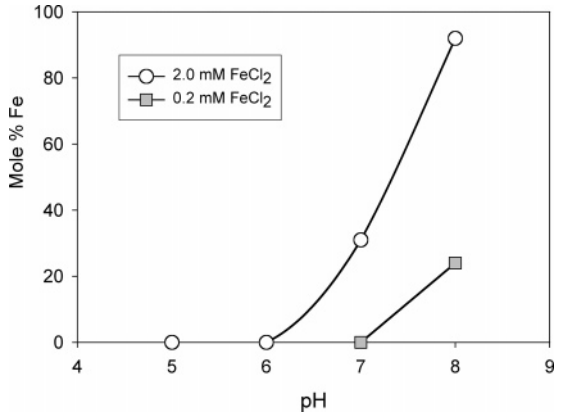

FIGURE 2. Influence of pH on magnetite precipitation upon reaction of 0.2 and 2.0 mM $FeCl_2$ with ferrihydrite-coated sand for 5 d.

In contrast to the impact of Fe(II) concentration on the extent of ferrihydrite conversion, the ligand does not impact the extent of ferrihydrite conversion following 132 h of reaction. The rates of ferrihydrite secondary mineralization, however, are a function of the ligand, being slower for chloride relative to sulfate, as noted for the precipitation of both goethite and lepidocrocite (Figure 1; Table 2). The influence of ligand type on the rate of goethite precipitation is a function of initial Fe(II) concentration (Figure 1; Table 2). Similar to lepidocrocite, the rate of goethite precipitation is approximately an order of magnitude slower in the presence of chloride relative to sulfate at low Fe(II) concentrations (0.2 mM). Conversely, at higher Fe(II) concentrations (2.0 mM), the rate of goethite precipitation is an order of magnitude faster for $FeCl_2$ than for $FeSO_4$. The rapid accumulation of goethite at the expense of lepidocrocite, however, decreases the rate of magnetite precipitation in the presence of sulfate (Table 2). Both ferrihydrite and goethite decline as magnetite levels increase, suggesting that some ferrihydrite is still accessible for conversion (Figure 1).

Addition of 10 mM bicarbonate alters the rate and operating secondary mineralization pathway upon ferrous sulfate reaction with ferrihydrite. Regardless of Fe(II) concentration, lepidocrocite precipitation is not observed following 5 d of reaction in the presence of bicarbonate (Table 1). Reaction of 0.2 and 2.0 mM ferrous sulfate with ferrihydrite results solely in the accumulation of goethite. While lepidocrocite may have been a precursor for goethite precipitation but was completely consumed following 5 d of reaction, we did not observe conversion of lepidocrocite-coated sand to goethite upon addition of Fe(II) in the presence of bicarbonate (see Supporting Information Table S1). Although magnetite is observed in the absence of bicarbonate upon reaction of 2 mM ferrous sulfate with ferrihydrite, in the presence of bicarbonate magnetite precipitation is inhibited (Table 1). Additionally, the rate of ferrihydrite conversion declines in the presence of bicarbonate. Upon addition of 0.2 mM Fe(II), 93% of ferrihydrite undergoes reductive dissolution and secondary mineralization in the absence of bicarbonate, while only 56% is transformed with bicarbonate (10 mM) present after 5 d of reaction.

Role of pH. The extent of magnetite precipitation varies as a function of pH (Figure 2), consistent with the reaction stoichiometry for ferrihydrite reaction with Fe(II).

$$2Fe(OH)_3 + Fe^{2+} = Fe_3O_4 + 2H_2O + 2H^+ \qquad (1)$$

Increasing the pH to 8 induces nearly complete conversion to magnetite upon reaction of 2 mM ferrous chloride with ferrihydrite after 5 d of reaction (Figure 2). Similarly, an increase in pH to 8 reduces the Fe(II) concentration required for magnetite precipitation by more than an order of magnitude (Figure 2). Conversely, at pH 6, magnetite does not precipitate within 5 d of reaction.

Discussion

Reaction of ferrous iron (as ferrous chloride) with 2-line ferrihydrite-coated sand results in the precipitation of goethite, lepidocrocite, and magnetite following 5 d of reaction at circumneutral pH (Figure 1; ref *6*; Supporting Information Figure S1). Upon initial reaction of Fe(II) with ferrihydrite, two competing reaction pathways ensue involving the reductive dissolution and conversion of ferrihydrite to either goethite or lepidocrocite. The formation of lepidocrocite and goethite occurs via Ostwald ripening of ferrihydrite (*1*). Iron(II) adsorption and electron transfer to structural Fe(III) enhances the dissolution rate and subsequent reprecipitation as a thermodynamically more stable phase. Lepidocrocite is observed as large (several micrometers) single-domain, tabular crystals having minor levels of ferrihydrite at crystal edges (Figure 3a,c). Goethite precipitates are dominantly observed originating from the ferrihydrite surface (Figure 3b). Upon goethite nucleation and growth from the ferrihydrite surface, Fe(II) sorption on the active goethite crystal face may allow for electron transfer through the goethite crystal and subsequent oxidation of Fe(II) on the goethite surface. Green rust (both soluble complexes and discrete precipitates) is commonly observed as a precursor to both goethite and lepidocrocite upon oxidation of Fe(II) solutions (*17*−*19*) and also as a secondary phase upon abiotic Fe(II) reaction and dissimilatory reduction of ferrihydrite (*20*). Green rust, however, was not observed in this study, suggesting that either precipitation of lepidocrocite did not proceed through a green rust precursor or that its residence time was shorter than the timing of our analysis.

The rate of lepidocrocite precipitation and dissolution is a function of Fe(II) concentration and ligand type, which subsequently influences the ensuing reaction pathways (Figures 1 and 4). Stabilization of lepidocrocite relative to goethite in the presence of chloride has been reported previously (*17*), and indeed we observe more extensive precipitation and longer residence times of lepidocrocite at high Cl concentrations, thus minimizing ferrihydrite conversion to goethite. In the absence of chloride, however, the precipitation of goethite is equal to (0.2 mM Fe(II); 0.67 mmol Fe(II)/g ferrihydrite) or greater than (2.0 mM Fe(II); 6.7 mmol Fe(II)/g ferrihydrite) that of lepidocrocite (Figure 1). Lepidocrocite is commonly found associated with goethite in noncalcareous soils (*1*). Lepidocrocite is, however, thermodynamically unstable with respect to goethite (*1*), and thus lepidocrocite may serve as a precursor to goethite formation. The transformation of lepidocrocite to goethite has been observed in both acidic and alkaline conditions (*21*, *22*). Correspondingly, the precipitation of goethite appears to form at the expense of lepidocrocite, especially at high Fe(II) concentrations in the absence of chloride (Figure 1). Furthermore, goethite precipitates are observed in suspension adjacent to lepidocrocite (Figure 3a). In fact, while reaction of Fe(II) with synthetic lepidocrocite does not result in substantial goethite precipitation upon reaction with both 0.2 and 2.0 mM $FeCl_2$, one-third of the lepidocrocite is converted to goethite at high Fe(II) concentrations in the absence of chloride (see Supporting Information Table S1). Accordingly, at higher Fe(II) concentrations (in the absence of Cl), lepidocrocite may rapidly convert to goethite and consequently may not be observed at longer reaction times (Figure 4).

The addition of bicarbonate favors the conversion of ferrihydrite to goethite (Table 1), yet it hinders the conversion of lepidocrocite to goethite upon addition of 2.0 mM $FeSO_4$

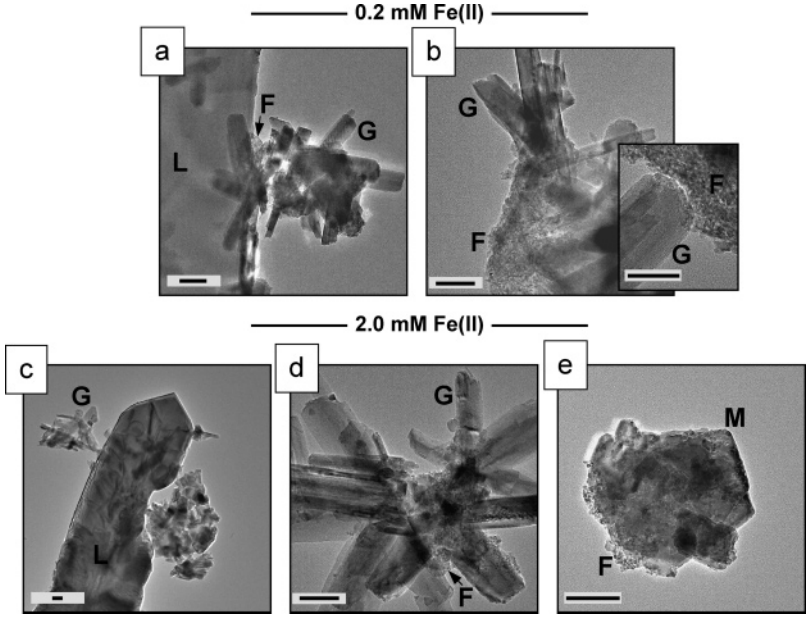

FIGURE 3. Transmission electron microscopy images of ferrihydrite, goethite, lepidocrocite, and magnetite following reaction of ferrihydrite with 0.2 (a,b) and 2.0 mM (c−e) $FeCl_2$ (pH 7.2). (a) Juxtapositioning of lepidocrocite, goethite, and ferrihydrite. (b) Goethite laths originating and growing out of ferrihydrite. Inset illustrates the interface between goethite and ferrihydrite. (c) Goethite flanking lepidocrocite. (d) Goethite twin with a ferrihydrite core. (e) Multidomainic magnetite crystal with ferrihydrite fringes. Scale bars equal 100 nm, except for the inset (b) scale is 50 nm.

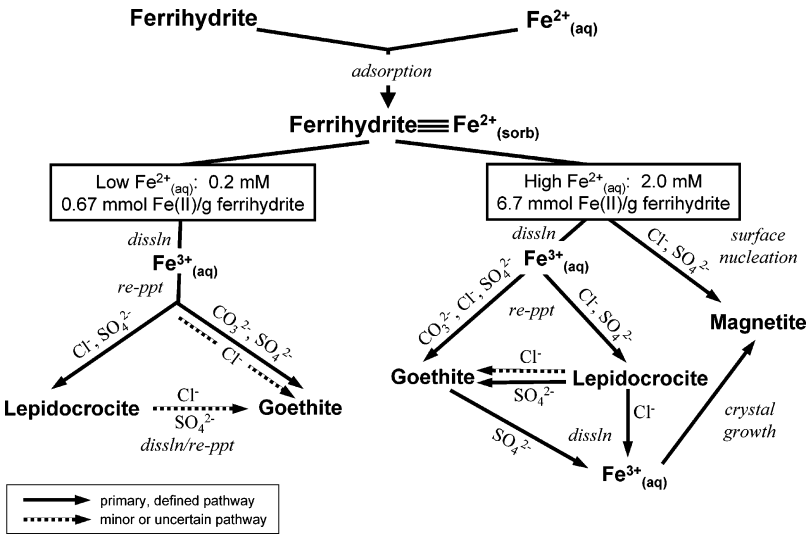

FIGURE 4. Conceptual model depicting the secondary phase transformation of ferrihydrite as a function of Fe(II) concentration and ligand (circumneutral pH). dissln = dissolution; re-ppt = reprecipitation. Rates for each conversion are reported in Table 2.

to lepidocrocite-coated sand (Supporting Information Table S1). The "goethite-favoring effect" of carbonate upon oxidation of Fe(II) in solution is well-documented (*1*, *23*−*25*). The proportion of goethite relative to lepidocrocite increases as the ratio of CO_2:O_2 increases (*1*, *25*). Goethite preference and subsequent lepidocrocite inhibition may be due to control of the spatial arrangement of the $[FeO_3(OH)_3]$ octahedral and suppression of nucleation of lepidocrocite in the presence of carbonate (*24*). Correspondingly, while goethite and lepidocrocite are both found within noncalcareous soils, lepidocrocite is absent in calcareous soils (*1*).

Following Fe(II) (>1.0 mmol Fe(II)/g ferrihydrite) reaction with ferrihydrite in the absence of carbonate, magnetite precipitation ensues (pH ≈ 7) (Figures 1 and 4). Interestingly, a mere one pH unit deviation from 7 either enhances (pH 8) or inhibits (pH 6) magnetite precipitation (Figure 2). Previously, magnetite precipitation was not observed following abiotic reaction of Fe(II) with ferrihydrite at concentrations high enough to induce siderite precipitation (*10*). Consistent with our findings, however, the authors propose that low pH conditions, a consequence of proton dislocation following Fe(II) sorption, may be responsible for the lack of magnetite precipitation (*10*). Upon reaction of Fe(II) with ferrihydrite, magnetite precipitates are observed, existing as large, multidomain cubic crystals with ferrihydrite fringes (Figure 3e). The formation of magnetite has been attributed to a structural conversion of ferrihydrite, induced by Fe(II) sorption and electron transfer to structural Fe(III) within ferrihydrite (*3*, *5*, *20*, *26*, *27*). Magnetite, being an inverse spinel, consists of Fe(II) in octahedral sites and Fe(III) in both tetrahedral and octahedral coordination (*1*). The presence of tetrahedral Fe(III) at the ferrihydrite surface has been proposed previously (*28*−*30*), yet its existence is not universally agreed upon (*29*−*34*). The nucleation of magnetite

may, in fact, be contingent upon the availability of surface tetrahedral Fe(III), thus explaining the heterogeneous distribution of magnetite on the ferrihydrite surface (*6*).

Goethite and lepidocrocite concentrations are lower at Fe(II) levels (>1.0 mmol Fe(II)/g ferrihydrite) conducive to magnetite nucleation and precipitation (Figure 1, Table 1). The conversion of lepidocrocite to magnetite in the presence of 0.1 M $FeSO_4$ solution (*35*) and in alkaline media has been suggested previously (*36*). Similarly, oxidation of Fe(II) in aerated solutions at pH 11 initially results in both goethite and magnetite, but goethite production ceases at early stages of oxidation, seemingly through the transformation to magnetite via a lepidocrocite precursor (*36*, *37*). The mechanism proposed for lepidocrocite transformation to magnetite involves the adsorption of Fe(II) species and interaction with the surface of lepidocrocite, similar to that proposed for the conversion of ferrihydrite to magnetite (*36*). However, we do not observe formation of magnetite following reaction of 2 mM Fe(II) with either goethite or lepidocrocite at circumneutral pH (see Supporting Information Table S1). Furthermore, high-resolution imaging of the surface of goethite (*12*) and lepidocrocite indicates no signs of magnetite nucleation (Figure 3). We have previously observed the inhibition of goethite precipitation by magnetite following dissimilatory reduction of ferrihydrite under advective flow (*6*). Upon magnetite nucleation, the dissolution/reprecipitation of ferrihydrite to goethite may decline as a result of magnetite's lower solubility and subsequent scavenging of Fe(III) (i.e., a decrease in Fe(III) activity).

As ferrihydrite becomes unavailable for reaction, further precipitation of magnetite is reliant upon the dissolution of goethite (SO_4) or lepidocrocite (Cl) to supply ferric iron for crystal growth on the ferrihydrite surface (Figure 1). The rapid conversion of lepidocrocite to goethite in the presence of sulfate decreases the rate and extent of magnetite accumulation (Table 2). The enhanced rate of goethite precipitation may be due to the rapid accumulation and conversion of lepidocrocite prior to the initiation of magnetite nucleation in the absence of chloride. Conversely, in the presence of chloride, the inhibition of lepidocrocite conversion to goethite allows for enhanced rates of magnetite precipitation (Table 2). We propose that this difference is a result of the higher solubility of lepidocrocite relative to goethite allowing for enhanced rates of magnetite crystal growth. Specifically, while ferrous iron and pH are the solution variables controlling magnetite nucleation (reaction 1 above), ferric iron must also be considered for crystal growth (reaction 2).

$$Fe^{2+} + 2Fe^{3+} + 4H_2O = Fe_3O_4 + 8H^+ \qquad (2)$$

Thus, lepidocrocite and/or goethite dissolution and subsequent Fe(III) activities may also contribute greatly to the crystal growth of magnetite upon exhaustion of reactive ferrihydrite surface sites (Figure 4), explaining the decline in goethite/lepidocrocite concentrations following magnetite nucleation (Figure 1; Supporting Information Figure S1).

In the presence of 10 mM bicarbonate, magnetite nucleation and precipitation is inhibited regardless of Fe(II) concentration (Table 1; Supporting Information Table S1). Similarly, the precipitation of magnetite following dissimilatory reduction of ferrihydrite is a function of the carbonate concentration in the medium (*3*, *5*). While magnetite is observed as a minor phase in an atmosphere of N_2:CO_2 with a ratio of 90:10, increasing the CO_2 proportion to 20% results in complete inhibition of magnetite precipitation (*5*). High bicarbonate concentrations may impede the structural conversion of ferrihydrite to magnetite as a result of aqueous complexation of Fe(II) or by minimizing site accessibility through bicarbonate sorption on the ferrihydrite surface (*5*). Conversely, we observe extensive magnetite precipitation following the reduction of ferrihydrite under advective flow in a bicarbonate-buffered (10 mM) medium (equivalent Fe(II) and bicarbonate concentrations to this study) (*11*). The removal of bicarbonate ions via solute transport may therefore relieve the inhibitory effects of carbonate sorption on ferrihydrite or diminish localized zones of elevated bicarbonate resulting from microbial respiration.

Secondary mineralization pathways following reaction of Fe(II) with ferrihydrite are complex and involve an interplay between a number of geochemical factors and competing Fe(II)-induced mineralization pathways (Figure 4). Lepidocrocite may be transient in most environments, yet it may play an important role in dictating the operative mineralization pathways of ferrihydrite. While the initial precipitation of goethite (especially in the presence of Cl) and magnetite is contingent upon Fe(II) reaction with ferrihydrite, the stability (i.e., residence time) of lepidocrocite appears to poise the system with respect to either goethite or magnetite. Regardless of Fe(II) concentration and ligand type, ferrihydrite is nearly completely consumed (82−94%) within 132 h of reaction. Considering the rapid and nearly complete conversion of ferrihydrite upon addition of even minor (ca. 40 μM) Fe(II) concentrations, the availability and/or long-term reactivity of ferrihydrite within mature environments is questionable.

Acknowledgments

We are very grateful to Alice Dohnalkova for her time and assistance in TEM analysis. TEM was performed in the Environmental Molecular Sciences Laboratory, a national scientific user facility sponsored by the Department of Energy's Office of Biological and Environmental Research (OBER), located at Pacific Northwest National Laboratory. This research was funded by the Natural and Accelerated Bioremediation Research (NABIR) program, Biological and Environmental Research (BER), U.S. Department of Energy (grant #DE-FG03-00ER63029). X-ray absorption spectroscopy was carried out at the Stanford Synchrotron Radiation Laboratory, a national user facility operated by Stanford University on behalf of the U.S. Department of Energy, Office of Basic Energy Sciences. The SSRL Structural Molecular Biology Program is supported by the Department of Energy, Office of Biological and Environmental Research, and by the National Institutes of Health, National Center for Research Resources, Biomedical Technology Program. We are also grateful to Associate Editor Janet Hering and three anonymous reviewers for their helpful comments and suggestions, which substantially strengthened the manuscript.

Supporting Information Available

Figure S1: The secondary mineralization of ferrihydrite as a function of initial Fe(II) concentration following 9 d of reaction at circumneutral pH. Table S1: A compiled list of mineral percentages following Fe(II) reaction with ferrihydrite, goethite, and lepidocrocite as a function of time, Fe(II) concentration, ligand, and pH. This material is available free of charge via the Internet at http://pubs.acs.org.

Literature Cited

(1) Cornell, R. M.; Schwertmann, U. *The Iron Oxides: Structure, Properties, Reactions, Occurrence and Uses*, 2nd ed.; VCH: Weinheim, Germany, 2003.

(2) Lovley, D. R.; Phillips, E. J. P. Availability of ferric iron for microbial reduction in bottom sediments of the freshwater tidal Potomac River. *Appl. Environ. Microbiol.* **1986**, *52*, 751−757.

(3) Fredrickson, J. K.; Zachara, J. M.; Kennedy, D. W.; et al. Biogenic iron mineralization accompanying the dissimilatory reduction of hydrous ferric oxide by a groundwater bacterium. *Geochim. Cosmochim. Acta* **1998**, *62*, 3239−3257.

(4) Glasauer, S.; Weidler, P. G.; Langley, S.; et al. Controls on Fe reduction and mineral formation by a subsurface bacterium. *Geochim. Cosmochim. Acta* **2003**, *67*, 1277−1288.
(5) Zachara, J. M.; Kukkadapu, R. K.; Fredrickson, J. K.; et al. Biomineralization of poorly crystalline Fe(III) oxides by dissimilatory metal reducing bacteria (DMRB). *Geomicrobiol. J.* **2002**, *19*, 179−207.
(6) Hansel, C. M.; Benner, S. G.; Neiss, J.; et al. Secondary mineralization pathways induced by dissimilatory iron reduction of ferrihydrite under advective flow. *Geochim. Cosmochim. Acta* **2003**, *67*, 2977−2992.
(7) Cornell, R. M.; Schneider, W. Formation of goethite from ferrihydrite at physiological pH under the influence of cysteine. *Polyhedron* **1989**, *8*, 149−155.
(8) Jang, J.-H.; Dempsey, B. A.; Catchen, G. L.; et al. Effects of Zn(II), Cu(II), Mn(II), Fe(II), NO_3^-, or SO_4^{2-} at pH 6.5 and 8.5 on transformations of hydrous ferric oxide (HFO) as evidenced by Mossbauer spectroscopy. *Colloids Surf., A* **2003**, *221*, 55−68.
(9) Fischer, W. R. Die Wirkung von zweiwertigem Eisen auf Losung und Umwandlung von Eisen(III)-hydroxiden. In *Pseudogley and gley Trans. Comm. V & VI*; Schlichting, E., Schwertmann, U., Eds.; VCH: Weinheim, 1972; pp 37−44.
(10) Fredrickson, J. K.; Kukkadapu, R. K.; Liu, C. K.; et al. Influence of electron donor/acceptor concentrations on hydrous ferric oxide (HFO) bioreduction. *Biodegradation* **2003**, *14*, 91−103.
(11) Benner, S. G.; Hansel, C. M.; Wielinga, B. W.; et al. Reductive dissolution and biomineralization of iron hydroxide under dynamic flow conditions. *Environ. Sci. Technol.* **2002**, *36*, 1705−1711.
(12) Hansel, C. M.; Benner, S. G.; Nico, P.; et al. Structural constrains of ferric (hydr)oxides on dissimilatory iron reduction and the fate of Fe(II). *Geochim. Cosmochim. Acta* **2004**, *68*, 3217−3229.
(13) Lovley, D. R.; Giovannoni, S. J.; White, D. C.; et al. *Geobacter metallireducens* gen. nov. sp. nov., a microorganism capable of coupling the complete oxidation of organic compounds to the reduction of iron and other metals. *Arch. Microbiol.* **1993**, *159*, 336−344.
(14) Lovley, D. R.; Woodward, J. C. Mechanisms for chelator stimulation of microbial Fe(III)-oxide reduction. *Chem. Geol.* **1996**, *132*, 19−24.
(15) Stookey, L. L. Ferrozine − a new spectrophotometric reagent for iron. *Anal. Chem.* **1970**, *42*, 779−781.
(16) George, G. N. EXAFSPAK: Stanford Synchrotron Radiation Laboratory, 1993.
(17) Taylor, R. M. Influence of chloride on the formation of iron oxides from Fe(II) chloride. Effect of (Cl) on the formation of lepidocrocite and its crystallinity. *Clays Clay Miner.* **1984**, *32*, 175−180.
(18) Lewis, D. G. Factors influencing the stability and properties of green rusts. *Adv. GeoEcol.* **1997**, *30*, 345−372.
(19) Schwertmann, U.; Fechter, H. The formation of green rust and its transformation to lepidocrocite. *Clay Miner.* **1994**, *29*, 87−92.
(20) Mann, S.; Frankel, R. B. Magnetite biomineralization in unicellular microorganisms. In *Biomineralization: Chemical and biochemical perspectives*; Mann, S., Webb, J., Williams, R. J. P., Eds.; VCH: Weinheim, 1989; pp 389−426.
(21) Bechine, K.; Subrt, J.; Hanslik, T.; et al. Transformation of synthetic g-FeOOH (lepidocrocite) in aqueous solutions of ferrous sulfate. *Z. Anorg. Allg. Chem.* **1982**, *489*, 186−196.
(22) Schwertmann, U.; Taylor, R. M. The transformation of lepidocrocite to goethite. *Clays Clay Miner.* **1972**, *20*, 151−158.
(23) Fey, M. V.; Dixon, J. B. Synthesis and properties of poorly crystalline hydrated aluminous goethites. *Clays Clay Miner.* **1981**, *29*, 91−100.
(24) Cornell, R. M.; Schneider, W.; Giovanoli, R. Phase transformations in the ferrihydrite/cysteine system. *Polyhedron* **1989**, *8*, 2829−2836.
(25) Carlson, L.; Schwertmann, U. The effect of CO_2 and oxidation rate on the formation of goethite versus lepidocrocite from an Fe(II) system at pH 6 and 7. *Clay Miner.* **1990**, *25*, 65−71.
(26) Tronc, E.; Belleville, P.; Jolivet, J. P.; et al. Transformation of ferric hydroxide into spinel by Fe(II) adsorption. *Langmuir* **1992**, *8*, 313−319.
(27) Cornell, R. M. The influence of some divalent cations on the transformation of ferrihydrite into more crystalline products. *Clay Miner.* **1988**, *23*, 329−332.
(28) Cardile, C. M. Tetrahedral Fe^{3+} in ferrihydrite: Fe Mossbauer spectroscopic evidence. *Clays Clay Miner.* **1988**, *36*, 537−539.
(29) Eggleton, R. A.; Fitzpatrick, R. W. New data and a revised structural model for ferrihydrite. *Clays Clay Miner.* **1988**, *36*, 111−124.
(30) Zhao, J.; Huggins, F. E.; Feng, Z.; et al. Ferrihydrite: Surface structure and its effects on phase transformation. *Clays Clay Miner.* **1994**, *42*, 737−746.
(31) Eggleton, R. A.; Fitzpatrick, R. W. New data and a revised structural model for ferrihydrite: Reply. *Clays Clay Miner.* **1990**, *38*, 335−336.
(32) Manceau, A.; Combes, J. M.; Calas, G. New data and a revised structural model for ferrihydrite: Comment. *Clays Clay Miner.* **1990**, *38*, 331−334.
(33) Manceau, A.; Gates, W. P. Surface structural model for ferrihydrite. *Clays Clay Miner.* **1997**, *45*, 448−460.
(34) Combes, J. M. Evolution de la structure locale des polymeres et gels ferriques lors de la cristallisation des oxydes de fer. Application au piegeage de Puranium: These Universite' Paris 6, Paris, 1988; p 193.
(35) Schwertmann, U.; Taylor, R. M. The in vitro transformation of soil lepidocrocite to goethite. *Pseudogley & Gley, Trans. Comm. V & VI*; Int. Soc. Soil Sci.: Stuttgart-Hohenheim, 1973; pp 45−54.
(36) Tamura, Y.; Ito, K.; Katsura, T. Transformation of γ-FeO(OH) to Fe_3O_4 by adsorption of iron (II) on on γ-FeO(OH). *J. Chem. Soc., Dalton Trans.* **1983**, *1983*, 189−194.
(37) Tamura, Y.; Buduan, P. V.; Katsura, T. Studies on the oxidation of iron(II) ions during formation of Fe_3O_4 and α-FeOOH by air oxidation of $Fe(OH)_2$ suspensions. *J. Chem. Soc., Dalton Trans.* **1981**, 1807−1811.

Received for review April 7, 2005. Revised manuscript received July 14, 2005. Accepted July 14, 2005.

ES050666Z